



**HAL**  
open science

## The drivers of dark diversity in the Scandinavian mountains are metric-dependent

Lore Hostens, Koenraad van Meerbeek, Dymphna Wiegmans, Keith Larson, Jonathan Roger Michel Henri Lenoir, Jan Clavel, Ronja Wedegärtner, Amber Pirée, Ivan Nijs, Jonas Lembrechts

### ► To cite this version:

Lore Hostens, Koenraad van Meerbeek, Dymphna Wiegmans, Keith Larson, Jonathan Roger Michel Henri Lenoir, et al.. The drivers of dark diversity in the Scandinavian mountains are metric-dependent. *Journal of Vegetation Science*, 2023, 34 (6), pp.e13212. 10.1111/jvs.13212 . hal-04423954

**HAL Id: hal-04423954**

**<https://hal.science/hal-04423954v1>**

Submitted on 31 Oct 2024

**HAL** is a multi-disciplinary open access archive for the deposit and dissemination of scientific research documents, whether they are published or not. The documents may come from teaching and research institutions in France or abroad, or from public or private research centers.

L'archive ouverte pluridisciplinaire **HAL**, est destinée au dépôt et à la diffusion de documents scientifiques de niveau recherche, publiés ou non, émanant des établissements d'enseignement et de recherche français ou étrangers, des laboratoires publics ou privés.

1 **The drivers of dark diversity in the Scandinavian mountains are metric-dependent**

2 *Lore Hostens<sup>1</sup>, Koenraad Van Meerbeek<sup>2,3</sup>, Dymphna Wiegmans<sup>1</sup>, Keith Larson<sup>4</sup>, Jonathan Lenoir<sup>5</sup>, Jan*  
3 *Clavel<sup>1</sup>, Ronja Wedegärtner<sup>6</sup>, Amber Piréer<sup>1</sup>, Ivan Nijs<sup>1</sup>, Jonas J. Lembrechts<sup>1</sup>*

4 Short title: Dark diversity can be metric-dependent

5 **Affiliations**

6 <sup>1</sup>Research Group Plants and Ecosystems (PLECO), University of Antwerp, Belgium

7 <sup>2</sup>Department Earth of Environmental Science, KU Leuven, Leuven, Belgium

8 <sup>3</sup>KU Leuven Plant Institute, KU Leuven, Leuven, Belgium

9 <sup>4</sup>Climate Impacts Research Centre, Department of Ecology and Environmental Sciences, Umeå  
10 University, Sweden

11 <sup>5</sup>UMR CNRS 7058, Ecologie et Dynamique des Systèmes Anthropisés (EDYSAN), Université de Picardie  
12 Jules Verne, Amiens, France

13 <sup>6</sup>Department of Biology, Norwegian University of Science and Technology, Trondheim, Norway

14 **Correspondence**

15 Lore Hostens, Research Group Plants and Ecosystems (PLECO), University of Antwerp, Belgium

16 Email: lore.hostens@kuleuven.be

17 Orcid: <https://orcid.org/0000-0001-8245-1152>

18 Jonas J. Lembrechts, Research Center Plants and Ecosystems (PLECO), University of Antwerp, Belgium

19 Email: jonas.lembrechts@uantwerpen.be

20 Orcid: <https://orcid.org/0000-0002-1933-0750>

21 **Funding information**

22 This project was funded by FWO projects G018919N, 12P1819N and W001919N, as well as by ANR-20-  
23 EBIS-0004, BiodivERsA, BiodivClim call 2019–2020.

24 **Abstract**

25 **Aim:** Dark diversity refers to the set of species that are not observed in an area but could potentially  
26 occur based on suitable local environmental conditions. In this paper, we applied both niche-based  
27 and co-occurrence-based methods to estimate the dark diversity of vascular plant species in the  
28 subarctic mountains. We then aimed to unravel the drivers explaining (1) why some locations were  
29 missing relatively more suitable species than others, and (2) why certain plant species were more often  
30 absent from suitable locations than others.

31 **Location:** The Scandinavian mountains around Abisko, northern Sweden.

32 **Methods:** We calculated the dark diversity in 107 plots spread out across four mountain trails using  
33 four different methods: two co-occurrence-based (Beals' index and hypergeometric method) and two  
34 niche-based (climatic niche model and climatic niche model followed by species-specific threshold)  
35 methods. We then applied multiple generalized linear mixed-effects models and general linear models  
36 to determine which habitat characteristics and species traits contributed the most to dark diversity.

37 **Results:** The study showed a notable divergence in the predicted drivers of dark diversity depending  
38 on the method used. Nevertheless, we can conclude that plot-level dark diversity was generally 17%  
39 higher in areas at low elevations and 31% higher in areas with a low species richness.

40 **Conclusion:** Our findings call for caution when interpreting statistical findings of dark diversity  
41 estimates. Even so, all analyses point towards an important role for natural processes such as

42 competitive dominance as the main driver of the spatial patterns found in dark diversity in the  
43 northern Scandes.

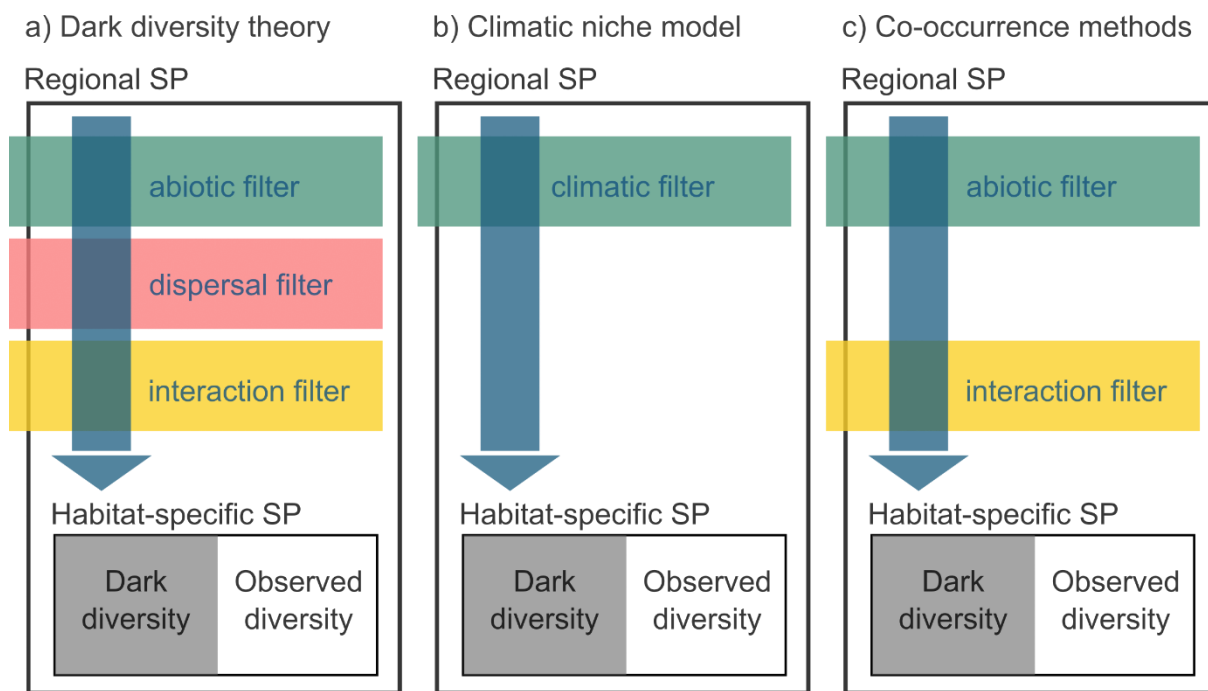
44 **Key-words:** plant ecology, Beals' index, co-occurrence-model, niche-model, method comparison, plant  
45 diversity, regional species pool, plant traits, habitat characteristics

## 46 **Introduction**

47 Terrestrial ecosystems are increasingly affected by land-use and climate change, leading to large-scale  
48 biodiversity loss and community turnover (Theurillat & Guisan, 2001; Mooney et al., 2009; Newbold et  
49 al., 2015). Biodiversity plays an important role in ecosystem health and its loss alters ecosystem  
50 function (Hooper et al., 2012; Tilman et al., 2014). While most research has focused on the set of  
51 species that occur in an area, much less attention has gone to those species that are missing but could  
52 potentially inhabit the area (Pärtel et al., 2011). Nevertheless, to get a better understanding of  
53 community patterns and their underlying processes, such species absences hold viable additional  
54 information (Pärtel, 2014). Knowing which species from the regional species pool are absent within a  
55 given locality and identifying why, can help fine-tune conservation planning (Lewis et al., 2017). For  
56 example, if many of the absent – yet expected based on climate conditions – species are dispersal  
57 limited or cannot access the focal area due to strong dispersal barriers (i.e., habitat fragmentation),  
58 then some form of facilitated dispersal through assisted migration or actions to restore habitat  
59 connectivity is needed to restore biodiversity. However, if the nutrient conditions in the soil of the  
60 focal area are unsuitable for many of the missing species, then only providing assisted migration  
61 towards climatically suitable locations or restoring suitable climatic corridors would not be sufficient  
62 as restoration measures.

63 Species belonging to the missing part of the environmentally filtered regional species pool are defined  
64 as the so-called “dark diversity” (see Figure 1a), a concept introduced by Pärtel et al. (2011). To be part  
65 of the dark diversity, the absent species must have a reasonable probability of dispersing to and  
66 establishing viable populations in the area (i.e., by belonging to the regional species pool) and its  
67 ecological requirements (depending on the methodology used that may incorporate either only its  
68 climatic or all environmental requirements) must match the local conditions (Pärtel, 2014). As a result,  
69 species that are present in the regional surroundings of the focal locality can be locally missing because  
70 they have a lower competitive ability, are dispersal limited, are ill-adapted to abiotic conditions, or due  
71 to stochastic processes (Keddy, 1992; Riibak et al., 2015). Understanding how extrinsic abiotic  
72 conditions and intrinsic species characteristics related to competition and dispersal abilities influence  
73 a species' absence can consequently give a better view of the community assembly (Belinchón et al.,  
74 2020).

75 The dark diversity concept does not encompass the total regional species pool across different habitats  
76 but focuses on the environmentally filtered, or habitat-specific, regional species pool (Lewis et al.,  
77 2017). Combining this habitat-specific regional species pool with the local observed species  
78 composition can result in an estimate of the dark diversity (Figure 1). However, there are several  
79 methods that use different biotic and abiotic filters to estimate the habitat-specific species pool (Figure  
80 1). Depending on the method, different outcomes can be expected, as explained below. One of the  
81 main benefits of the dark diversity concept is that it enables us to compare biodiversity across various  
82 habitats or ecosystems despite significant differences in local diversity by deriving a relativized  
83 biodiversity index from the dark diversity, known as community completeness (Pärtel et al., 2011;  
84 Pärtel et al., 2013).



85

86 *Figure 1: Schematic overview of three approaches used to estimate the habitat-specific species pool (SP). a) the theoretical*  
 87 *concept of dark diversity, where the dark diversity is the non-observed set of species in a certain location, after filtering the*  
 88 *regional species pool based on abiotic, dispersal and biotic interaction limitations. In b), dark diversity is calculated using*  
 89 *climatic filtering of the regional species pool (e.g. using climatic niche models to estimate which species could occur at a*  
 90 *certain location), while c) represents commonly used co-occurrence-based methods, which integrate both abiotic and*  
 91 *interaction filters. Figure adjusted from Stephenson (2016). The combination of dark- and observed diversity encompasses the*  
 92 *habitat-specific species pool. Note that for both the methods in b) and c), several other methodological decisions can still be*  
 93 *made that might affect the outcome.*

94 Estimating dark diversity is not straightforward but can be done in multiple ways (Lewis et al., 2016,  
 95 Figure 1). The difficulty lies in estimating the habitat-specific species pool, which is, as explained above,  
 96 the set of species in a region that can persist in the environmental conditions of the target site (Pärtel  
 97 et al., 2011). It encompasses both the observed and dark diversity of the focal habitat. One could  
 98 perform extensive sampling of habitat types in a region to estimate the habitat-specific species pool  
 99 of each habitat type but this can be costly and time-consuming (de Bello et al., 2016). Therefore,  
 100 computational approaches are often implemented. Most commonly, two types of methods are used  
 101 to estimate the habitat-specific species pool, either (1) based on the abiotic niche of the species (e.g.,  
 102 using ecological indicator values or species distribution models) or (2) based on metrics of species'  
 103 co-occurrence (e.g., the Beals' probability index or the hypergeometric method) (Lenoir et al., 2010; de  
 104 Bello et al., 2016; Carmona and Pärtel, 2020).

105 Ecological indicator values are a proxy for species' ecological requirements and are often used to  
 106 characterize environmental conditions. The approach allows to identify species from the regional  
 107 species pool along environmental gradients based on their ecological preferences (Ellenberg et al.,  
 108 1991). A downside of this method is the difficulty of defining the realized niche of species since such  
 109 indicator values are rough estimates of the niche optimum along a few specific ecological gradients,  
 110 often based on expert knowledge (Lewis et al., 2016). Potentially more accurate approaches based on  
 111 abiotic conditions make use of habitat suitability models to estimate species' environmental niches  
 112 (Guisan & Thuiller, 2005). These models can be used to determine the environmental conditions  
 113 suitable for a species (Parolo et al., 2008). In this method, the accuracy of the models highly depends  
 114 on the resolution as well as on the selected set of environmental data (de Bello et al., 2016).  
 115 Additionally, predicting a species' habitat suitability based only on occurrence observations and

116 environmental data may prove to be difficult since processes like competition can play a crucial role,  
117 especially at the local scale (Cadotte & Tucker, 2017).

118 In both the above-mentioned methods, the aim is to estimate the suitability of a location based only  
119 on the environmental niche of the species, regardless of the other species co-occurring in said location.  
120 By contrast, one could also estimate the potential of finding a species at a certain location based on  
121 the presence of its associated species. The Beals' probability index can be used to calculate species co-  
122 occurrence patterns (Beals, 1984). It relies on the idea that the presence of a species that is frequently  
123 found together with another species could indicate shared suitable abiotic conditions (Ewald, 2002). If  
124 the associated species of a target species are observed, but the target species itself is not, it is part of  
125 the dark diversity. The hypergeometric method works similarly by verifying if certain species  
126 associations occur more often than predicted by chance and by estimating the dark diversity of a given  
127 species at a location from the likelihood of its co-occurrence with species present at that location  
128 (Carmona & Pärtel, 2020). The major difference between the Beals' probability index and  
129 hypergeometric method is that the hypergeometric method compares the actual number of co-  
130 occurrences between two species to the association of random pairs of species (i.e. under the  
131 assumption that there is no association). The difference between the observed and random  
132 association provides the index value, whereas for the Beals' index, the index value is only based on the  
133 observed patterns of co-occurrence (Carmona & Pärtel, 2020; Trindade et al., 2023). The advantage of  
134 these two co-occurrence-based approaches is that one only requires species composition data in the  
135 community without the need for environmental conditions. However, the prediction of the probability  
136 of a given species to belong to the dark diversity is dependent on the distribution of other species,  
137 which is especially challenging for species that are not strongly confined to particular communities or  
138 for environments where traditional communities and thus species associations are truncated (e.g., due  
139 to habitat disturbances).

140 All these methods share a common purpose: they help recognize species that belong to the habitat-  
141 specific species pool. The species not recorded in the observed diversity, but belonging to the habitat-  
142 specific species pool of the focal site are part of the dark diversity (Figure 1; Pärtel et al., 2011).  
143 Considering the absence of a standard method for calculating the habitat-specific species pool and, by  
144 extension, the dark diversity, we used both niche- and co-occurrence-based approaches. Our aim was  
145 to estimate the dark diversity around Abisko, Sweden. We wanted to explore whether these different  
146 methods would yield varying estimates of dark diversity due to their inherent filters (Figure 1). We  
147 then further explored the drivers behind the spatial patterns of this dark diversity and assessed the  
148 impact of the different methods on these drivers. The concept of dark diversity is still in its infancy and  
149 therefore only a handful of studies have explored why species are part of the dark diversity, none of  
150 which were to our knowledge conducted in subarctic environments (Belinchón et al., 2020; Moeslund  
151 et al., 2017; Riibak et al., 2015). In this study, we wanted to unravel the drivers behind (1) why some  
152 locations are missing relatively more suitable species than others, and (2) why certain vascular plants  
153 of the Scandinavian mountains are more often absent from suitable locations than others.

154 In light of the first research question, we expected locations with a higher relative dark diversity,  
155 hereafter referred to as plot-level dark diversity (i.e., a higher percentage of missing species from the  
156 habitat-specific species pool) to: (1) appear at lower elevations, as more intense competition will  
157 exclude a higher proportion of species (Jones & Gilbert, 2016); (2) be at the extreme ends of  
158 disturbance gradients, based on the intermediate disturbance hypothesis (Lembrechts et al., 2014;  
159 Rashid et al., 2021); (3) be at the extreme end of low pH and/or moisture gradients, since such  
160 conditions can be tolerated by a few species only (Gough et al., 2000; Vonlanthen et al., 2006); or (4)  
161 have low observed species richness, as these locations will be dominated by highly competitive species

162 preventing specialist species from co-occurring (Pellissier et al., 2010). Of course, these factors would  
163 act in addition to the stochasticity that always explains part of the variation in species occurrences at  
164 small spatial scales (Mohd et al., 2016).

165 The composition of dark diversity can be influenced by not only plot characteristics but also species  
166 traits. Certain traits might make some species more likely to be absent from plots, thereby contributing  
167 to the dark diversity (Moeslund et al., 2017). Therefore, we have selected six species traits related to  
168 resource-use efficiency and dispersal as these can play a key factor in plant recruitment and  
169 persistence. We predict that plant species with a higher dark diversity probability, hereafter referred  
170 to as species-level dark diversity (i.e., absent in a higher percentage of plots where they were predicted  
171 to occur) to: (1) have a higher specific leaf area (SLA), since the soils in the alpine habitats of the study  
172 area are nutrient-poor (Westoby, 1998); (2) have a lower maximum vegetative plant height, as smaller  
173 plants would be more easily outcompeted in plots were they could theoretically occur; (3) have a  
174 higher seed mass or short-distance dispersal, since these are (loosely) correlated to a limited dispersal  
175 ability and lower seed abundance, which decreases the number of successful dispersal events (Howe  
176 & Smallwood, 1982; Ozinga et al., 2005); (4) be more recently introduced in the region, as non-native  
177 species have a more limited distribution and show possible time-lags in niche filling (Alexander et al.,  
178 2016; Crooks, 2005); or finally, (5) be associated with arbuscular mycorrhizal (AM) or ectomycorrhizal  
179 (EcM) fungi, as the native vegetation in the region is dominated by ericoid mycorrhizal (ErM) species  
180 (Finlay, 2008; Tedersoo, 2017).

## 181 **2 Materials and methods**

### 182 **2.1 Study area**

183 The field data collection was performed in July and August 2021 in the Abisko area, northern Sweden  
184 (68°21'N, 18°49'E). The region has a subarctic montane climate with an average annual temperature  
185 of -0.6°C (1913-2020, although average annual temperatures have not dropped below 0°C since 2011)  
186 and average annual precipitation of 310 mm (Abisko Scientific Research Station, 400 m above sea level  
187 (a.s.l.); <https://polar.se/>). The soil is comprised of till, colluvium, and glacio-fluvial deposits (Callaghan  
188 et al., 2013). At high elevations, the area is covered in snow for about 27 weeks of the year (Callaghan  
189 et al., 2013). At low elevations, the vegetation is dominated by open birch forests (*Betula pubescens*  
190 Ehrh.), with additional presence of rowan (*Sorbus aucuparia* L.) and several willow species (*Salix* sp.).  
191 The understory vegetation often consists of heath species (e.g., dwarf birch (*Betula nana* L.), European  
192 blueberry (*Vaccinium myrtillus* L.) and black crowberry (*Empetrum nigrum* L.)), or meadow species  
193 (e.g., Alpine bistort (*Bistorta vivipara* L.), globeflower (*Trollius europaeus* L.) and Alpine saw-wort  
194 (*Saussurea alpina* DC.)) (Sonesson & Lundberg, 1974). Above the treeline (520 m a.s.l), the vegetation  
195 is dominated by alpine/arctic heathland species (e.g., blue heath (*Phyllodoce caerulea* L.), bog  
196 blueberry (*Vaccinium uliginosum* L.) and lingonberry (*Vaccinium vitis-idaea* L.)) (Kullman, 2015).

### 197 **2.2 Field data collection**

#### 198 **2.2.1 Study sites**

199 A total of 107 plots were surveyed in the vicinity of four mountain trails: Björkliden, Låktatjåkka, Nuolja,  
200 and Rallarvägen (Figure 2).



201

202 *Figure 2: Map of the study area around Abisko, Sweden (grey dot on the inset), with 107 surveyed plots*  
 203 *along the four hiking trails (colors) and the different survey methods (symbols).*

204 Data from new and ongoing vegetation surveys were combined, with two different methodologies: 73  
 205 1 m × 1 m plots from a long-term vegetation composition monitoring project in the area (hereafter  
 206 called ‘small plots’), as well as 34 large (10 m × 10 m) plots established in the framework of the global  
 207 DarkDivNet network (Pärtel et al., 2019). Of the 107 plots, 40 were situated along trails close to  
 208 Björkliden and around Låktatjåkka (Wedegärtner et al., 2022), 57 in the Abisko National Park on Mount  
 209 Nuolja (MacDougall et al., 2021), and 10 along the Rallarvägen.

## 210 **2.2.2 Large plots**

211 The vegetation monitoring method used in the large plots was based on the DarkDivNet protocol  
 212 (Pärtel et al., 2019). The plots (10 m × 10 m) were placed at a 10 m perpendicular distance from the  
 213 trail. In each plot, all vascular plants were recorded. Species were identified using the Fjällflora  
 214 (Mossberg & Stenberg 2008). Observations that could not be identified to the species level (e.g.,  
 215 *Alchemilla* sp.) were removed from the species list and thus also from the regional species pool.  
 216 Furthermore, following the DarkDivNet protocol, the maximum vegetative height (cm) was measured  
 217 with a ruler for the tallest individual of each species in all plots.

218 In every plot, we visually estimated the cover (%) of total vegetation, bare ground, rock, litter,  
 219 herbaceous vegetation, bryophytes, lichen, shrubs, and trees (> 200 cm). At the center of every plot,  
 220 the exact location was recorded with a hand-held GARMIN GPSMAP® 66i GPS receiver. Soil samples  
 221 were collected using the protocol explained below (see 2.3).

## 222 **2.2.3 Small plots**

223 The small plots were surveyed using the pin-point or point intercept method, which is often used to  
224 assess plant cover (Jonasson, 1988). A 1 m × 1 m plot was placed at 10 m from the trail. In one plot,  
225 100 pins were vertically dropped in 10 cm increments from left to right and top to bottom. With every  
226 pin-drop, we recorded the vascular plant species touching the pin, multiple recordings for the same  
227 species occurred when more than one individual of that species touched the pin. When the pin  
228 touched only the ground, the observation was categorized as either litter, bryophytes, bare soil, or  
229 lichen, a single hit was noted. Soil samples were collected using the same protocol as explained below  
230 (see 2.3).

### 231 **2.3 Soil sample analysis**

232 Soil samples were collected in 50 out of the 107 plots (both large and small plots). During sampling,  
233 the litter covering the soil was removed and a minimum of 300 g of soil was taken from the top 10 cm  
234 of the ground. Soil samples could not be collected along the Nuolja trail (57/107 plots) as this trail is in  
235 the Abisko National Park and no sampling permission was obtained in the year of the survey. However,  
236 50 of these plots were long-term permanent plots for which soil pH measurements were available from  
237 previous soil sampling campaigns conducted in 2018 (using the same sampling and analysis  
238 procedure). The seven remaining plots were in very close (<10 m) proximity to small plots for which  
239 pH was measured in 2018, and we therefore used the mean pH of those plots. Ultimately, pH could be  
240 obtained for all but one plot, assuming that when largely undisturbed – as was the case in the system  
241 – pH-values would only change slightly over time.

242 All soil samples were stored in a fridge at 4°C until they were analyzed between September and  
243 December 2021 at the University of Antwerp, Belgium. To measure soil pH, 25 mL of a KCl solution was  
244 added to 10 g (9.9-10.1 g) of soil. The samples were put in a shaker for an hour and afterward rested  
245 for another 60 min. Then, soil pH was measured with a 914 pH/Conductometer by Metrohm© in the  
246 liquid layer at the top of the sample after shortly manually shaking the tubes.

### 247 **2.4 Online data collection**

#### 248 **2.4.1 Gridded data products**

249 To create the climatic niche models, we collected gridded climate data with a resolution of 30  
250 arcseconds (c. 1 km at the equator) for annual mean air temperature, annual precipitation, mean  
251 maximum air temperature of the warmest month, and mean minimum air temperature of the coldest  
252 month. Gridded data were downloaded from CHELSA version 1.2, representing the long-term (1979-  
253 2013) climatic conditions (Karger et al., 2017).

254 Soil temperature estimates (i.e., annual mean soil temperature, mean soil minimum temperature of  
255 the coldest month and mean soil maximum temperature of the warmest month) were obtained from  
256 the SoilTemp global maps of soil temperature (Lembrechts et al., 2021). The SoilTemp maps were  
257 derived from CHELSA monthly air temperature maps and the offset between gridded air temperature  
258 and in-situ soil temperature measurements stored in the SoilTemp database (Lembrechts et al. 2020).  
259 The gridded data, representative of the upper soil layer (top 5 cm), had the same resolution as the  
260 CHELSA data, namely 30 arcseconds.

261 Elevation was extracted from the European Digital Elevation Model (DEM) with a resolution of 25 m,  
262 obtained from Copernicus Land Monitoring Service version 1.1 (European Union, 2021).

263 Lastly, the topographic wetness index, a topographical proxy for soil moisture, was obtained from a  
264 TWI raster layer covering Europe (Haesen et al., 2021). The TWI raster, which had a spatial resolution  
265 of 25 m, was generated using the method developed by Kopecký et al. (2021).



266 All gridded data were handled in R version 4.2.1 (R Core Team, 2021) using the raster (Hijmans et al.,  
267 2012), sp (Pebesma et al., 2005), and rgdal (Keitt et al., 2010) packages to overlay the spatial  
268 coordinates of all 107 plots and extract climatic information at the plot-level.

#### 269 **2.4.2 Type of disturbance**

270 For every plot, we assigned a type of disturbance based on its proximity to hiking trails, roads, and  
271 railroad. By visual assessment in QGIS, one of the three disturbance types (hiking trail, road or railroad)  
272 was assigned to every plot (QGIS Development Team, 2021). All plots were close to hiking trails, yet  
273 whenever the railroad or a road was within 150 m of the plot, its impact was considered dominant,  
274 and the hiking trail classification thus overruled. While a continuous variable for distance to the  
275 disturbance would have allowed for more nuance, adding a separate parameter for distance to the  
276 trail, to the road and to the railroad was not possible, as all plots were at a fixed distance of 10 m from  
277 a trail, and the distance to road and railroad were too strongly correlated.

#### 278 **2.4.3 Amount of bare ground**

279 Disturbances can generate patches of bare ground that can open empty niches for new species to  
280 colonize and establish themselves (Lembrechts et al., 2014). The amount of bare ground (%), here used  
281 as a proxy of disturbance, was estimated or calculated for every plot. For the large plots, this was  
282 estimated from the percentage cover of litter and bare ground. This was calculated for the small plots  
283 by summing up all the pins that touched bare ground and litter, dividing this by the total number of  
284 pins in a plot.

#### 285 **2.4.4 Plant functional traits**

286 Average maximum vegetative plant height per species was calculated from the measurements done in  
287 the large plots.

288 The specific leaf area (SLA) for every species was retrieved from data collected in the framework of the  
289 Mountain Invasion Research Network (MIREN) in the region in 2017 (published as part of the Tundra  
290 Trait Team database (TTT); Bjorkman et al., 2018). The SLA was calculated as leaf area (cm<sup>2</sup>)/dry weight  
291 (g).

292 Average seed mass per species was obtained from the global TTT database or – if not available there -  
293 the LEDA Traitbase (Bjorkman et al., 2018; Kleyer et al., 2008).

294 The dispersal type per species was also retrieved from the LEDA Traitbase and used to categorize  
295 species according to their potential for long-distance dispersal (LDD) and short-distance dispersal (SDD)  
296 (Kleyer et al., 2008). All species were considered long-distance dispersers, hence this variable was not  
297 included in further analyses.

#### 298 **2.4.5 Nativeness Index**

299 We used a continuous rather than a binary measure of the status of a species within a region, to get a  
300 more accurate view of the history of the species. Our nativeness index (NI) used historical surveys from  
301 the Global Biodiversity Information Facility ([GBIF](#)) database. It considered the first year a species was  
302 observed (year first occurrence species) and the first year in which more than 50 species were  
303 observed in the region (year first survey). If the NI was close to 1, the species was already observed at  
304 the time of the first survey. As the value approached 0, the species was observed increasingly recently  
305 for the first time and was thus more likely to be non-native.

306 
$$NI = \frac{\sqrt{\text{year (2020)} - \text{year first occurrence species}}}{\sqrt{\text{year (2020)} - \text{year first survey (1850)}}$$

307 Square roots were used in the formula to give more weight to recent differences (e.g., a first  
308 observation in 2010 vs 2020 is considered a more substantial difference than one in 1900 vs 1910). The  
309 first occurrence and the year of the first survey were obtained using the *rgbif* package (Chamberlain  
310 et al., 2021).

311 Note that the region was poor in non-native species, and those present were mostly introduced  
312 already over a century ago (Wiegmans et al., 2022). This is reflected in the high values of our nativeness  
313 index (mean = 0.98, 5% lowest = 0.88). Consequently, one should not expect strong effects of  
314 nativeness on dark diversity patterns in the northern Scandes.

#### 315 **2.4.6 Mycorrhizal associations**

316 The association of plant species with the main types of mycorrhizal fungi (AM = arbuscular mycorrhiza,  
317 EcM = ectomycorrhiza, ErM = ericoid mycorrhiza and NM = no mycorrhiza) was retrieved from the  
318 FungalRoot database (Soudzilovskaia et al., 2020).

319 More details on the online data collection can be found in Appendix S1.

### 320 **2.5 Data-analysis**

#### 321 **2.5.1 Dark diversity modeling**

322 For further analysis, only species with 10 or more occurrences, were included (n=49), as sufficient  
323 observations were needed to calibrate climatic niche models and build co-occurrence matrices. We  
324 then used the same dataset in four different approaches to estimate dark diversity. All statistical  
325 analyses were conducted in R version 4.2.1 (R Core Team, 2021).

#### 326 Climatic niche modeling

327 The presence and absence of all species in every plot was used to make climatic niche models. For  
328 every species, a generalized linear model (GLM; Bates et al., 2015) was calibrated, with a binomial  
329 distribution containing all climatic variables and their quadratic terms as explanatory variables (i.e.,  
330 annual mean air temperature, annual precipitation, maximum air temperature of the warmest month,  
331 minimum air temperature of the coldest month, annual mean soil temperature, minimum soil  
332 temperature of the coldest month, and maximum soil temperature of the warmest month) and  
333 presence/absence (1/0) of a species per plot as the response variable. Multicollinearity was checked  
334 using the Variance Inflation Factor (VIF) from the *car* package (Fox & Weisberg, 2011) and variables  
335 that increased the VIF to 5 or more were removed. The final models contained: annual precipitation,  
336 minimum soil temperature of the coldest month, maximum soil temperature of the warmest month,  
337 and their quadratic terms. No further model selection was done as we were not interested in a model  
338 identifying the drivers of the species' climatic niche, but rather wanted to approximate their climatic  
339 niche as consistently as possible.

340 To predict the probability of a species' occurrence in a specific plot, the GLM was calibrated on all  
341 remaining plots (Lembrechts et al., 2019) and the probability was estimated for that specific plot  
342 excluded from the model calibration. This leave-one-out procedure was then repeated for all plots and  
343 all species, each time predicting the probability of occurrence of a species in a plot based on a model  
344 calibrated on its occurrence pattern in all other plots. We then calculated the relative dark diversity  
345 per plot by averaging the predicted presence of each absent species in a plot and the dark diversity

346 probability per species by averaging the predicted presence of a species across all plots where it was  
347 absent.

348 The second method to estimate the dark diversity used the same climatic niche model as above. Yet,  
349 instead of continuous probability estimates, we converted niche model predictions into  
350 presence/absence estimates. For this, we calculated species-specific thresholds for presence using the  
351 function *ecospat.max.tss* from the *ecospat* package (Broennimann et al., 2022) which chooses the  
352 threshold that maximizes values for the True Skill Statistic (TSS), which assesses the accuracy of species  
353 distribution models (Allouche et al., 2006). Based on this, we created a binary dataset where the values  
354 below the threshold got a 0 (predicted to be absent) and the values above got a 1 (predicted to be  
355 present). Afterward, we removed the values where the species was observed to be present based on  
356 the vegetation surveys. To calculate the species-level dark diversity probability, we used the formula  
357 proposed by Moeslund et al. (2017), using the number of plot-level observations and predictions:

$$358 \frac{\# \text{ times in dark diversity}}{\# \text{ times in species pool}}$$

359 To calculate the relative plot-level dark diversity:

$$360 \frac{\# \text{ species in dark diversity}}{\# \text{ species in species pool}}$$

361 The habitat-specific species pool consisted of both the observed and dark species. Note that at the  
362 species level, we are estimating the probability that a species belongs to the dark diversity (dark  
363 diversity probability), while at the plot-level, we are estimating the percentage of species from the  
364 species pool that is absent (dark diversity *per se*).

#### 365 Beals' method

366 Two co-occurrence-based methods to estimate the dark diversity were used, with the first being the  
367 Beals' index (Beals, 1984), as applied by Lewis et al. (2016). We first built a species co-occurrence  
368 matrix, then calculated the Beals' index, using the *beals* function from the *vegan* package, for each  
369 species in every plot, excluding the focal species as suggested by Oksanen et al. (2022). The thresholds  
370 used to decide whether a species was part of the regional species pool were species-specific and  
371 defined as the 5th percentile of the Beals' index value for the species (Gijbels et al., 2012). Before  
372 calculating each threshold, the lowest value of the Beals' index was determined among the plots  
373 containing occurrences of the species in question, and all plots with values below this lowest value  
374 were discarded (Moeslund et al., 2017). For each plot, the dark diversity then consisted of all species  
375 from the habitat-specific species pool, except those present (Pärtel et al., 2011). To calculate the plot-  
376 and species-level dark diversity probability the same formulae as for the species-specific threshold  
377 were used.

#### 378 Hypergeometric method

379 The second method used to estimate the dark diversity was the hypergeometric method, as proposed  
380 by Carmona & Pärtel (2020). This method avoids the binary form in which dark diversity is often  
381 defined. The co-occurrence matrix used for the Beals' method was also employed in this case. To get  
382 estimates of the dark diversity, we used the function *DarkDiv* from the *DarkDiv* package, with the  
383 argument 'method' containing 'Hypergeometric' (Carmona & Pärtel, 2020). We applied this method  
384 to all species in all plots for which we obtained a probability that the species could be present in that  
385 plot. Afterward, all values for plots where the species were observed to be present were removed and  
386 a conservative threshold of 0.9 was applied as done by Trindade et al. (2023). All values below 0.9 were

387 given a 0 since we did not expect the species to be present here. To calculate the relative plot-level  
388 dark diversity, per plot the mean was taken from the remaining values (i.e. all values larger than 0.9).  
389 The same was done for the species-level dark diversity, yet here the mean was taken per species.

### 390 **2.5.2 Drivers of relative plot-level dark diversity**

391 To investigate why certain plots had a higher relative dark diversity, we created generalized linear  
392 mixed-effects models (GLMMs) with a beta distribution and logit-link function using the *glmmTMB*  
393 package (Brooks et al., 2017). Predictions from each of the four dark diversity indices (the two  
394 approaches based on niche models, the Beals' index, and the hypergeometric approach) were used as  
395 the response variable.

396 These plot-level models contained elevation, soil pH, type of disturbance, amount of bare ground, TWI,  
397 observed species richness and plot size as explanatory variables. The plots were situated along various  
398 trails. To account for this hierarchical sampling design, the model included a random intercept for plot  
399 number nested within trail identity. Multicollinearity and distribution of residuals were checked using  
400 the Variance Inflation Factor (VIF) and the *DHARMA* package (Hartig, 2022) and deemed not violated.  
401 Due to the low sample size, we limited ourselves to linear patterns and did not include two-way  
402 interaction terms since these more complex models could not converge. For the same reason,  
403 quadratic effects were not tested, even though theoretically they could be expected for pH and soil  
404 moisture. However, within our study system both the pH and moisture gradient only reached extreme  
405 values on one side of the gradient (e.g., highly acidic yet no highly basic soils).

406 No further model selection was performed (Hartig, 2018). The variance explained by the full model  
407 was obtained using the *performance* function from the *performance* package (Lüdecke et al., 2021).  
408 To determine the proportion of explained variance of every variable, we followed a variation  
409 partitioning approach. First, the variance of the full model was calculated. Afterward, for every  
410 explanatory variable, a model was made consisting of all variables except the focal variable. By  
411 extracting the marginal  $R^2$  of the individual models from the  $R^2$  of the full model, the variance of the  
412 focal variable was obtained (Legendre & Legendre, 1998). Community completeness was also  
413 calculated for each plot and every method as  $\ln(\text{observed richness}/\text{dark diversity})$  (Pärtel et al., 2013).  
414 A linear mixed model was created using the *lmer* function from the *lme4* package (Bates et al., 2015)  
415 with plot as a random factor to compare whether the community completeness differed significantly  
416 depending on the method. The distribution of the residuals was checked using the *DHARMA* package  
417 (Hartig, 2022) and assumptions were not deemed violated. As one needs to assess community  
418 completeness using species numbers, the community completeness based on the climatic niche  
419 models had to be calculated using a species-specific threshold as well, thus resulting in the same values  
420 as in the original dark diversity assessment using climatic niche models with a threshold. We thus  
421 maintained only one of these in the comparison.

### 422 **2.5.3 Drivers of species-level dark diversity probability**

423 To investigate why certain species had a higher dark diversity probability, we created GLMs with a beta  
424 distribution and logit-link function using the *betareg* package (Cribari-Neto & Zeileis, 2010) with  
425 predictions from each of the used dark diversity indices (based on the niche models, the Beals' index,  
426 and the hypergeometric approach) as a response variable.

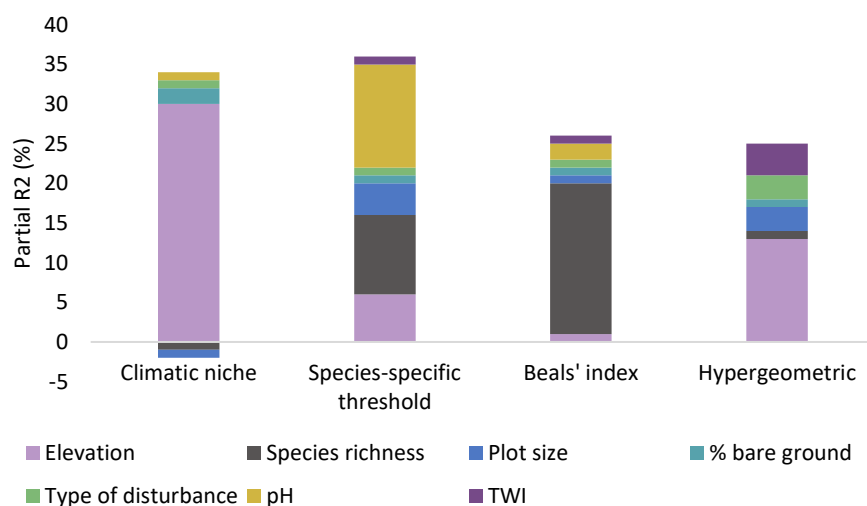
427 First, full models were made separately for each dark diversity index that contained the nativeness  
428 index, maximum vegetative plant height, specific leaf area, dispersal type, seed mass, and mycorrhizal  
429 association as explanatory variables and species-level dark diversity as the response variable.  
430 Assumptions of multicollinearity and distribution of residuals were tested and not violated. Here as

431 well, two-way interaction terms could not be tested and no further model selection was performed  
 432 (Hartig, 2018). Afterward, pairwise comparisons were conducted on the categorical parameters using  
 433 the *emmeans* package (Lenth, 2022).

### 434 3 Results

#### 435 3.1 Plot-level dark diversity

436 Depending on the method, we could explain between 39% and 87% of the variance in plot-level dark  
 437 diversity. In two cases (climatic niche models and hypergeometric method), elevation was responsible  
 438 for the largest share, while in the two other cases (species-specific threshold and Beals' index) species  
 439 richness was the most dominant factor (Figure 3). On average across all models, elevation explained  
 440 13% of the variance, species richness 7%, and plot size, type of disturbance, amount of bare ground,  
 441 pH and TWI explained an additional 2%, 1%, 2%, 4% and 2%, respectively. Note that due to the nature  
 442 of the variance partitioning calculations, variances do not necessarily add up to the total variance of  
 443 the full model.



444

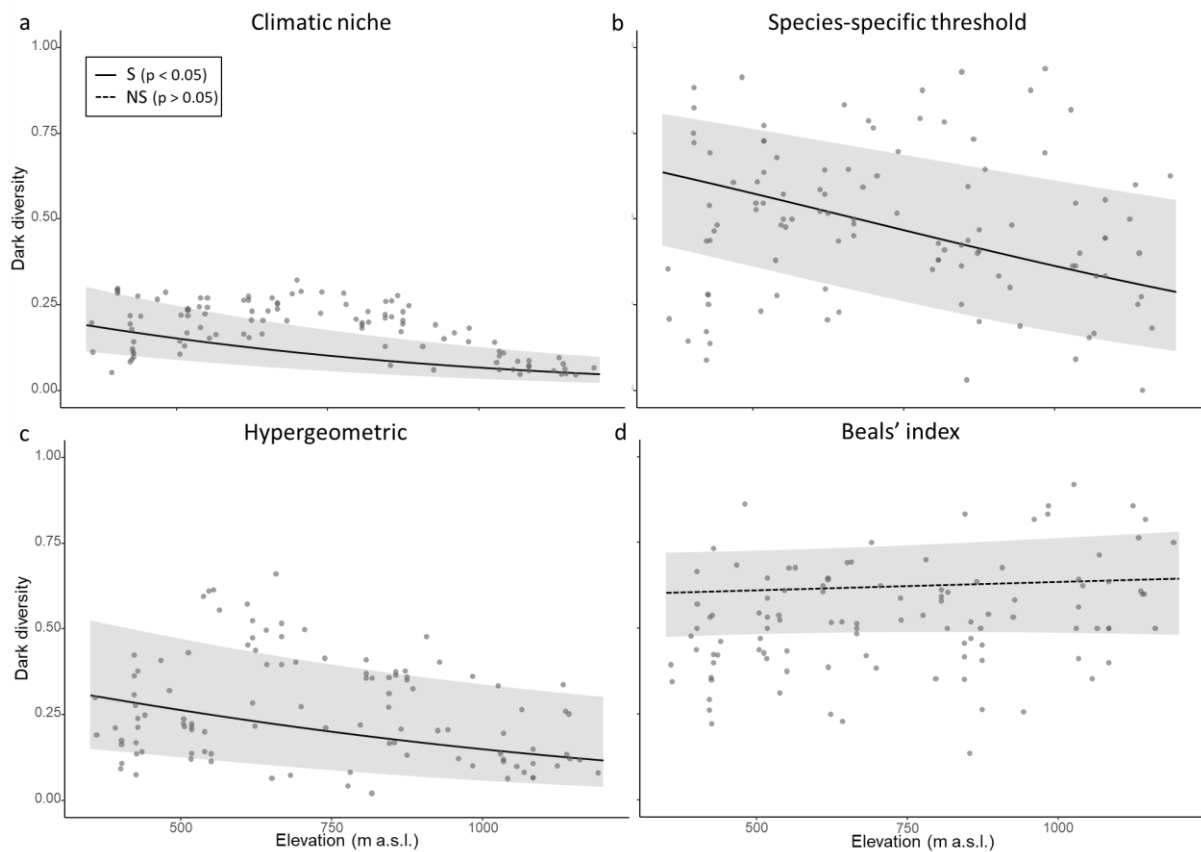
445 *Figure 3: Variance partitioning (expressed in % and calculated using the marginal R<sup>2</sup>) of the different*  
 446 *explanatory variables in the GLMMs of the plot-level analyses on the predictions of each of the four*  
 447 *different dark diversity methods. TWI = topographic wetness index.*

448 In three out of the four methods used, the plot-level dark diversity decreased significantly across the  
 449 elevation gradient (Table 1; Figure 4). Only in the model based on the Beals' index did elevation not  
 450 have a significant influence (Table 1; Figure 4d).

451 *Table 1: Models explaining the plot-level dark diversity using the different dark diversity estimation*  
 452 *methods: coefficients (p-values: \* p<0.05; \*\* p<0.01; \*\*\* p<0.001). The factor used for the intercept*  
 453 *was allocated alphabetically and all other factors were compared to this baseline. Beals = Beals' index;*  
 454 *CN = climatic niche models; Hyper = hypergeometric method; SS = species-specific threshold; Elev =*  
 455 *elevation; SR = species richness; TOD = type of disturbance; TWI = topographic wetness index.*

Model	Intercept (Road)	Elev	SR	Plot size (10m x 10m)	TOD Hiking trail	TOD Railroad	% bare ground	pH	TWI	AIC
Beals	1.04*	10 <sup>-4</sup>	-0.082** *	-0.121	-0.112	-0.345	0.001	0.032	0.001	-195
CN	-0.327	-0.001***	-0.029** *	0.079	0.524	-0.251	-0.001*	-0.022	-0.014	-370
Hyper	0.101	-0.001**	0.01	-0.304	0.416	-0.177	-0.006	-0.001	-0.071	-137
SS	3.00***	-0.001**	-0.105** *	-0.408*	0.281	-0.165	-0.001	-0.262* **	0.038	-140

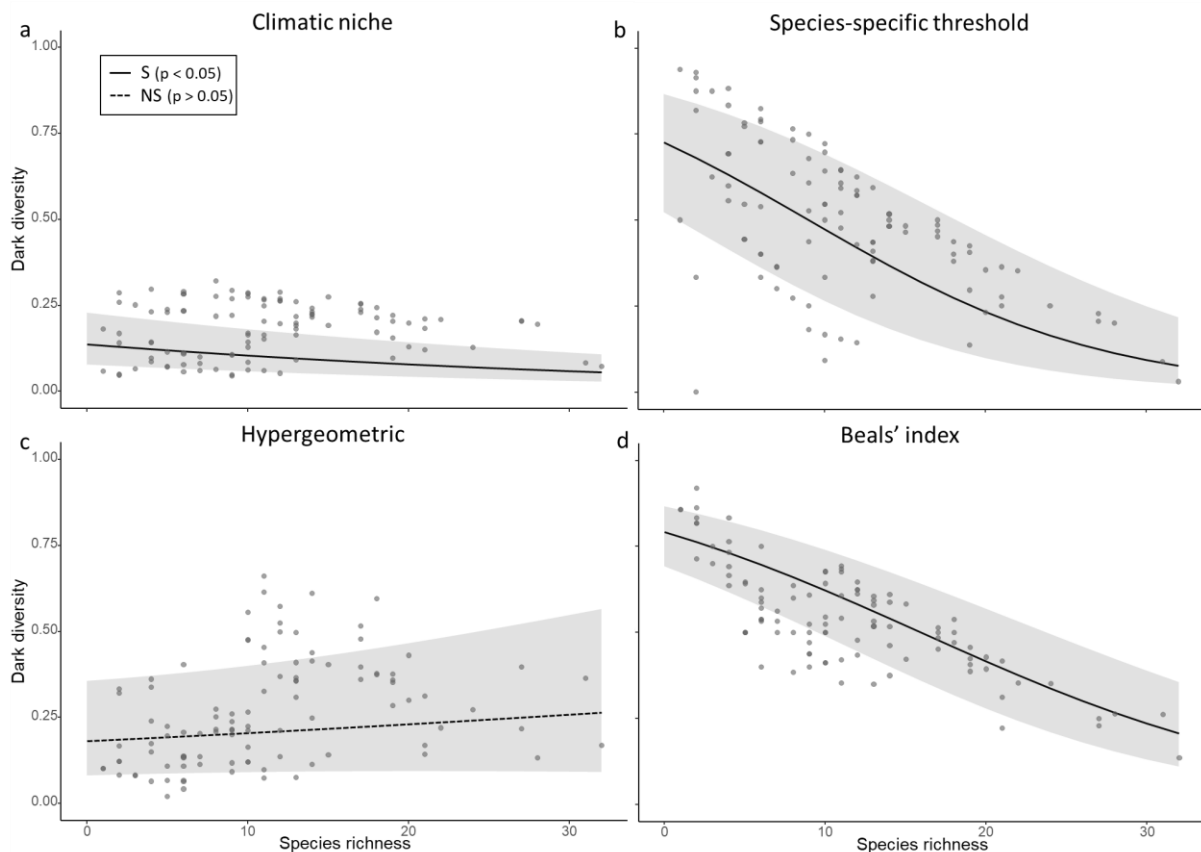
456



457  
 458 *Figure 4: Marginal effects plots of the plot-level dark diversity as a function of elevation (m a.s.l.). The*  
 459 *grey area indicates the 95% confidence interval and the grey dots are the raw data points. Dark*  
 460 *diversity was estimated using a) the climatic niche models, b) the climatic niche models followed by the*  
 461 *species-specific threshold, c) the hypergeometric method and d) the Beals' index. S = significant; NS =*  
 462 *non-significant.*

463 The plot-level dark diversity decreased significantly with increasing species richness in three cases  
 464 (Table 1; Figure 5a, 5b, 5d), yet increased with increasing species richness when using the  
 465 hypergeometric method, albeit not significantly (Table 1; Figure 5c).

466



467  
 468 *Figure 5: Marginal effects plots of the plot-level dark diversity as a function of species richness. The*  
 469 *grey area indicates the 95% confidence interval, and the grey dots are the raw data points. a) the*  
 470 *climatic niche models, b) the climatic niche models followed by the species-specific threshold, c) the*  
 471 *hypergeometric method and d) the Beals' index. S = significant; NS = non-significant.*

472 Furthermore, our results indicate that only the climatic niche model had a significant relationship  
 473 between dark diversity and bare ground. Moreover, only the climatic niche model followed by the  
 474 species-specific threshold had significant relationships with plot size and pH (Appendix S2, Figure S1a).  
 475 In the remaining two models, none of the other variables were found to be significant predictors of  
 476 dark diversity.

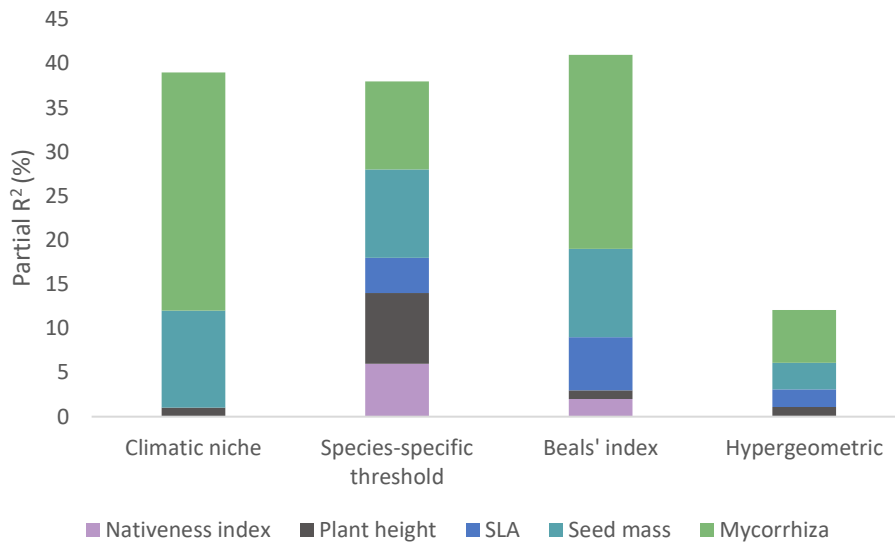
477 Lastly, the community completeness based on the Beals' index was significantly lower than the  
 478 community completeness based on the other two methods (Appendix S2, Figure S2).

### 479 **3.2 Species-level dark diversity**

480 Depending on the method, we could explain between 8% and 45% of the variance in species-level dark  
 481 diversity (Figure 6). In all cases, mycorrhizal association was responsible for the largest share (Figure  
 482 6). On average across all models, mycorrhizal association explained 16% of the variance, seed mass  
 483 9%, SLA 3% and the NI and the maximum vegetative plant height an additional 2% and 3%, respectively.  
 484 Note that due to the nature of the variance partitioning calculations, variances do not necessarily add  
 485 up to the total variance of the full model.

486





487

488 *Figure 6: Variance partitioning (expressed in % and calculated using the marginal R<sup>2</sup>) of the different*  
 489 *explanatory variables in the GLMs of the species-level analyses on the predictions of each of the four*  
 490 *different dark diversity methods. SLA = specific leaf area.*

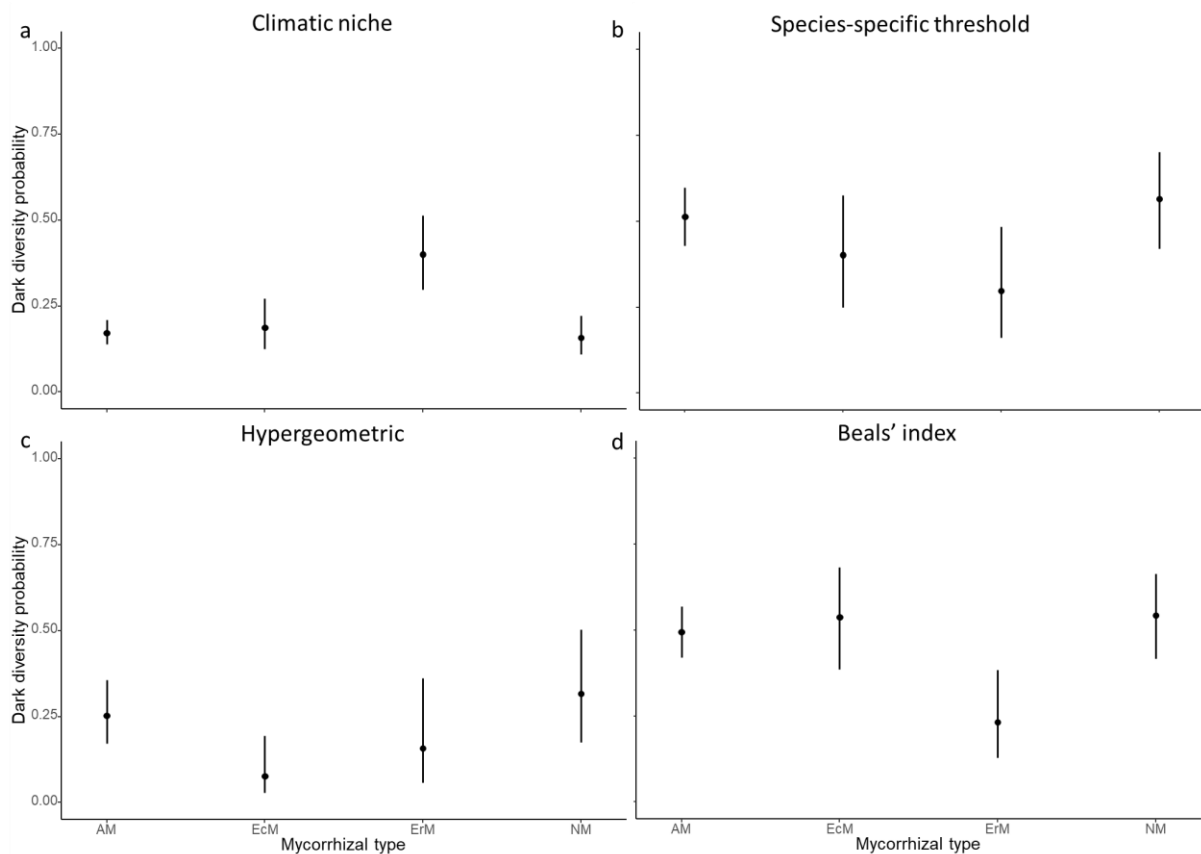
491 Mycorrhizal status was the only significant parameter in the climate niche model approach, with  
 492 ericoid mycorrhizae differing significantly from AM, EcM and NM (Figure 7; Table 2; Appendix S3).  
 493 Species with a symbiotic ericoid mycorrhizal association had a significantly higher dark diversity than  
 494 all other associations when using the climatic niche models (Table 2; Figure 8a). However, the opposite  
 495 was true when using the Beal's index and climatic niche model followed by the species-specific  
 496 threshold (Table 2; Figure 7b, d). For the Beals' index the contrast test also revealed that ericoid  
 497 mycorrhizae differed significantly from AM, EcM and NM (Figure 7d, Appendix S3). For the species-  
 498 specific threshold, the contrast test only showed a borderline significant difference between ErM and  
 499 NM (Figure 7b; Appendix S3). Lastly, and even more contrasting, species with a symbiotic  
 500 ectomycorrhizal association had a significantly lower dark diversity than all other associations when  
 501 using the hypergeometric method (Figure 7c). The contrast test also revealed that EcM differed  
 502 significantly from AM and NM (Appendix S3).

503 *Table 2: Models explaining the plot-level dark diversity using the different dark diversity estimate*  
 504 *methods: coefficients (p-values: \* p<0.05; \*\* p<0.01; \*\*\* p<0.001). The factor used for the intercept*  
 505 *was allocated alphabetically and all other factors were compared to this baseline. Beals = Beals' index;*  
 506 *CN = climatic niche models; Hyper = hypergeometric method; SS = species-specific threshold; AM =*  
 507 *arbuscular mycorrhiza; EcM = ectomycorrhiza; ErM = ericoid mycorrhiza; NM = no mycorrhiza; MVH =*  
 508 *maximum vegetative plant height; SLA = specific leaf area; NI = nativeness index; SM = seed mass.*

Model	Intercept (AM)	EcM	ErM	NM	MVH	SLA	NI	SM	AIC
Beals	1.04*	0.170	-1.17***	0.193	-10 <sup>-4</sup>	-0.001	-3.28	-0.089	-19

CN	-0.043	0.108	1.17***	-0.101	-10 <sup>-4</sup>	-10 <sup>-4</sup>	-1.37	-0.068	-72
Hyper	-3.66	-1.40*	-0.597	0.314	0.001	-0.001	3.42	0.121	-38
SS	-5.96	0.453	-0.916*	0.208	-0.001	-0.001	6.95	0.082	-11

509



510

511 *Figure 7: Prediction of the species-level dark diversity in relation to the mycorrhizal type based on the*  
512 *beta regression model. The black dots show the average dark diversity per individual factor whereas*  
513 *the error bars show the standard deviation. AM = arbuscular mycorrhiza; EcM = ectomycorrhiza; ErM*  
514 *= ericoid mycorrhiza; NM = no mycorrhiza. Dark diversity estimated using a) the climatic niche models,*  
515 *b) species-specific threshold, c) the hypergeometric method and d) the Beals' index.*

516

None of the other variables had a significant influence on the species-level dark diversity.

517

#### 4. Discussion

518

##### 4.1. Plot-level dark diversity

519 We found relatively consistent patterns in the drivers of dark diversity at the plot-level, but much less  
520 consistency was observed at the species level. Plot-level dark diversity was most consistently related  
521 to elevation, with plots at higher elevations having a lower plot-level dark diversity - and thus fewer  
522 expected species missing - than plots at lower elevations. This was true for both niche-based methods  
523 as well as for the hypergeometric method, yet not for the Beals' index, in which elevation was not  
524 significant. Such a decline with elevation is in line with ecological theory. Indeed, under harsh  
525 environmental conditions, competitive interactions are often replaced by mutualistic ones, or  
526 competition is at least lowered in intensity, thereby reducing the exclusion of less competitive species  
527 with a lower dark diversity as a result (Callaway et al., 2002; Klanderud, 2010; Lembrechts et al., 2018).  
528 Additionally, the presence of more ruderal and competitive species in the lowlands compared to the  
529 stress-tolerant species higher up in the mountains along roadsides also suggests that reduced  
530 competition can be one of the main drivers behind the lower dark diversity at higher elevations  
531 (Lembrechts et al., 2014). Furthermore, climatic conditions are usually milder in the lowlands, making  
532 them suitable for a broader set of species (Körner, 2021). Consequently, since more species can be  
533 present in these plots, it is also more likely that at least some of them are excluded, resulting in a  
534 higher number of species belonging to the dark diversity. As the co-occurrence-based metrics  
535 accounted for some of these factors (e.g., lower expectancy of species in plots dominated by species  
536 that traditionally outcompete them), it should come as no surprise that elevation was not significant  
537 in the model for the Beals' index.

538 Species richness was identified as a key driver of plot-level dark diversity in three out of the four  
539 methods. Its effect was negative for all but the hypergeometric method for which it was not significant,  
540 thus largely following our hypothesis. In this system, plots with a low number of species are likely to  
541 be dominated by highly competitive species, which can prevent the establishment of several species  
542 that could in theory occur there (Pellissier et al., 2010). Indeed, plots with a low species richness in the  
543 study system were often dominated by *Empetrum nigrum*. It is an efficient competitor for nutrients,  
544 can grow on soils with low pH, and has allelopathic effects against seed germination and the growth  
545 of surrounding species (Tybirk et al., 2000), and can possibly direct several species from the regional  
546 species pool locally to the dark diversity. Our results seem to support the study by Fløjgaard et al.  
547 (2020) who found that competitive species have an adverse effect on species richness, leading to an  
548 increase in dark diversity. Nevertheless, it is possible that approaches based on species co-occurrences,  
549 such as the hypergeometric method and the Beals' index, already account for this effect of  
550 competition.

551 Finally, the amount of bare ground, soil pH and plot size also appeared to have a significant effect on  
552 the plot-level dark diversity, but this was only the case for the niche-based methods. No other variables  
553 were significant for the other two methods which already indicates that these models should be  
554 handled with caution.

#### 555 **4.2 Species-level dark diversity**

556 Mycorrhizal association was the only variable with significant influence, across all methods, on the  
557 species-level dark diversity across all methods. However, while species with a symbiotic ericoid  
558 mycorrhizal association had a significantly higher dark diversity than all other associations when using  
559 the climatic niche models, the opposite was true for the climatic niche model followed by a species-  
560 specific threshold and the Beals' method. Noteworthy, when using the hypergeometric method  
561 species with a symbiotic ectomycorrhizal association had a significantly lower dark diversity than all  
562 other associations. These contrasting results highlight the differences between the different methods  
563 used to estimate dark diversity. In the Scandinavian mountains, the species with an ErM association

564 (e.g. *E. nigrum* and *V. vitis-idaea*) were virtually not climate-limited (occurring in 64 and 63 out of the  
565 107 plots, respectively) and could in theory, based on their climatic niche, be present in all plots.  
566 Therefore, their dark diversity probability ended up being very high in any plot where they were  
567 absent, simply because of the underlying modeling approach. We aimed to correct this issue by using  
568 species-specific thresholds, yet here again mycorrhizal type was withheld as significant.

569 These ErM-associated species not only dominated the studied landscape, but they were also often  
570 found in strong association with each other, resulting in clear predictions of their presence once one  
571 of them was present, when using the Beals' index. As their spatial connection in the field was so  
572 consistent, their estimated dark diversity using these methods ended up relatively low. Additionally,  
573 as ErM-fungi are the most dominant and widespread fungi in tundra regions (Tendersoo, 2017), in  
574 theory, there ought to be enough coverage of ErM-fungi so that the establishment of species  
575 associated with them should not be hampered. Consequently, there should be less reason for the  
576 species to be absent in areas where they could potentially occur than for AM-associated species  
577 (Tendersoo, 2017). All of this suggests that the observed higher dark diversity estimates for ErM-  
578 associated species based on the climatic niche approach are most likely a methodological artefact.  
579 These methodological issues could also explain why such little consistency was observed for the other  
580 studied drivers of species-level dark diversity, calling for caution when interpreting findings from any  
581 such dark diversity estimate separately.

#### 582 **4.3 Comparison of methods and uncertainties**

583 In this paper, we estimated dark diversity using both niche-based and co-occurrence-based methods,  
584 which are often used interchangeably in the scientific literature. However, our results suggest that  
585 both approaches have significantly different assumptions and, as a result, get relatively incomparable  
586 results. Indeed, the niche-based approaches estimate the dark diversity as the set of species that could  
587 occur at a certain location based on their climatic niche or other environmental filters. The latter  
588 drivers are then often used as explanatory variables for the observed dark diversity, as done in the  
589 underlying study. For example, reduced competitive interactions in sites with larger percentages of  
590 bare ground would result in lower dark diversity, as is hinted at by our results.

591 Co-occurrence-based methods, on the other hand, estimate dark diversity simply from the neighboring  
592 species with which a target species is usually associated. These approaches incorporate biotic  
593 interactions inherently in the dark diversity estimate. However, they do exclude species from the dark  
594 diversity for which the climatic conditions fall within their climatic limits, yet whose co-occurring  
595 species are also missing at a site. The latter could be especially problematic in diverse communities  
596 with high beta diversity, or areas with truncated, reduced, or novel communities as a result of  
597 anthropogenic land use or climatic changes (Christensen et al., 2021).

598 Perhaps more worryingly, within each type of dark diversity estimation method, results were not  
599 necessarily in agreement with each other. We found largely different findings, especially for species-  
600 level dark diversity, when using climatic niches with or without species-specific thresholds, as well as  
601 when using the hypergeometric method versus the Beals' index. Additionally, the community  
602 completeness also differed significantly, depending on the method used. As such, our results highlight  
603 the need for caution and transparency when calculating and interpreting dark diversity estimates, as  
604 the conclusions depend heavily on the methodological decisions one makes, and methods should thus  
605 be tailored to the specific research questions.

606 Of course, several alternative methods could still be used to estimate dark diversity, and many  
607 adjustments to the methods used above could be proposed. For example, one could use global  
608 datasets such as GBIF to model the climatic niche, rather than data from the study region only. Using  
609 global datasets for such broader-scale niche models could result in a more accurate estimate of the  
610 climatic niche since the entire climatic niche could be modelled, rather than a truncated version as  
611 results from regional data (Bazzichetto et al., 2023). However, most of these global datasets lack  
612 absence data and presences are obtained using a wide variety of methodologies and spatial resolutions  
613 (Tessarolo et al., 2014), while abiotic data is at the global scale often only available at coarser resolution  
614 (Lembrechts et al., 2019). This could also make the predictions less accurate. Additionally, there is the  
615 possibility of mismatches, especially for rare species, since global datasets can be spatially biased  
616 (Meyer et al., 2016). Therefore, predicting local climatic niches based on global data can make it more  
617 difficult to figure out whether the absences are due to a bias in the global dataset or the drivers under  
618 investigation. Furthermore, it is worth mentioning that alternative thresholds could be used for the  
619 species-specific method, such as Cohen's Kappa or Area Under the Curve (AUC). The chosen TSS  
620 threshold in this study may be affected by the low prevalence of species (Leroy et al., 2018). However,  
621 since we only used the relatively common species, the issue of low prevalence should not pose a  
622 notable concern (Allouche et al., 2006; Wunderlich et al., 2019). These alternative threshold methods  
623 were not examined in this particular study as this may further complicate methodological decisions for  
624 dark diversity estimation. Hence, we suggest that more research is needed to investigate the impact  
625 of alternative thresholds when using species-specific methods.

626 The most promising avenue could perhaps come from an approach that combines both climatic niches  
627 with co-occurrences, such as joint Species Distribution Models (jSDMs; Pollock et al., 2014). This recent  
628 class of distribution models draws information from species co-occurrences and explains spatial  
629 variation in species distributions by extending standard species distribution models with species–  
630 species associations. Such an approach could potentially allow distinguishing through one model  
631 between absences driven by environmental unsuitability, biotic interactions, or other drivers.  
632 Nevertheless, Carmona & Pärtel (2020) did find that jSDMs could not outperform the hypergeometric  
633 method, yet they do substantially increase computational time.

#### 634 **4.5 Conclusions**

635 The concept of dark diversity is still in its infancy, yet its contribution to understanding community  
636 completeness and its use in nature conservation has already been shown to be significant (Lewis et al.,  
637 2017; Riibak et al., 2015). In this context, it is crucial to determine whether a species' absence is a  
638 result of species-specific traits or plot characteristics, be it abiotic factors or biotic interactions, which  
639 is something traditional biodiversity studies that only focus on species presences cannot provide. We  
640 here compared different methodological approaches to estimate dark diversity and showed significant  
641 divergence in predicted drivers of dark diversity based on the method used, calling for caution when  
642 interpreting statistical findings on dark diversity estimates. Given the high level of variation in outcome  
643 between methods, it is currently not possible to recommend one or the other. More comparative  
644 studies in different environments are thus necessary to elaborate further on the search for a robust  
645 methodology to estimate dark diversity. Nevertheless, we can generally conclude that areas at low  
646 elevations, and, to a certain extent, with a low species richness showed a higher plot-level dark  
647 diversity, largely due to natural processes such as competitive dominance. How valid these findings  
648 are for patterns in dark diversity in other (mountain) areas across the globe remains to be seen, yet  
649 the significant effect of methodological decisions on conclusions should remind us that any other  
650 regional study on dark diversity should be cautious in its conclusions. Nonetheless, one could assume

651 that dark diversity will indeed decrease with increasing elevation since only more specialized species  
652 can survive at higher elevations, and competition is lower.

### 653 **Acknowledgments**

654 We thank the master students Renée Lejeune and Jasmine Spreewers for their assistance in gathering  
655 data during the summer of 2021. Additionally, we extend our appreciation to Stef Haesen for supplying  
656 us with the raster layer for the topographic wetness index (TWI).

### 657 **Author contribution**

658 J.J.L. and L.H. conceived the research idea; L.H., D.W. and J.C. collected data; L.H. performed statistical  
659 analyses with guidance from J.J.L.; L.H. and J.J.L. wrote the paper with contributions from K.V.M.; all  
660 authors discussed the results and commented on the manuscript.

### 661 **Data availability statement**

662 All data and codes that support the findings of this study are available on Zenodo  
663 <https://zenodo.org/record/8059877>.

### 664 **References**

- 665 Alexander, J. M., Lembrechts, J. J., Cavieres, L. A., Daehler, C., Haider, S., Kueffer, C. et al., (2016)  
666 Plant invasions into mountains and alpine ecosystems: current status and future challenges.  
667 *Alpine Botany*, 126, 89–103. <https://doi.org/10.1007/s00035-016-0172-8>
- 668 Allouche, O., Tsoar, A., & Kadmon, R. (2006) Assessing the accuracy of species distribution models:  
669 prevalence, kappa and the true skill statistic (TSS). *Journal of applied ecology*, 43, 1223–1232.  
670 <https://doi.org/10.1111/j.1365-2664.2006.01214.x>
- 671 Bates, D., Mächler, M., Bolker, B., Walker, S. (2015) Fitting linear mixed-effects models using  
672 lme4. *Journal of Statistical Software*, 67, 1–48. doi:10.18637/jss.v067.i01
- 673 Bazzichetto, M., Lenoir, J., Da Re, D., Tordoni, E., Rocchini, D., Malavasi, M. et al. (2023) Sampling  
674 strategy matters to accurately estimate response curves' parameters in species distribution  
675 models. *Global Ecology and Biogeography*. <https://doi.org/10.1111/geb.13725>
- 676 Beals, E. W. (1984) Bray-curtis ordination: An effective strategy for analysis of multivariate ecological  
677 data. *Advances in Ecological Research*, 14, 1–55. <https://doi.org/10.1111/oik.07308>
- 678 Belinchón, R., Hemrová, L., & Münzbergová, Z. (2020) Functional traits determine why species belong  
679 to the dark diversity in a dry grassland fragmented landscape. *Oikos*, 129, 1468–1480.  
680 <https://doi.org/10.1111/oik.07308>
- 681 Bjorkman, A. D., Myers-Smith, I. H., Elmendorf, S. C., Normand, S., Thomas, H. J. D., Alatalo, J. M. et al.  
682 (2018) Tundra Trait Team: A database of plant traits spanning the tundra biome. *Global*  
683 *Ecology and Biogeography*, 27, 1402–1411. <https://doi.org/10.1111/geb.12821>
- 684 Broennimann, O., Di Cola, V., Guisan, A. (2022). *Ecospat: spatial ecology miscellaneous methods*.  
685 *Version 3.4*. Available at <https://CRAN.R-project.org/package=ecospat> [Accessed 16 March  
686 2022]
- 687 Brooks, M. E., Kristensen, K., van Benthem, K. J., Magnusson, A., Berg, C. W., Nielsen, A. et al.  
688 (2017) “glmmTMB Balances Speed and Flexibility Among Packages for Zero-inflated  
689 Generalized Linear Mixed Modeling.” *The R Journal*, 9, 378–400.
- 690 Cadotte, M. W., Tucker, C. M. (2017) Should environmental filtering be abandoned? *Trends in ecology*  
691 *and evolution*, 32, 429–437. <https://doi.org/10.1016/j.tree.2017.03.004>

692 Callaghan, T. V., Jonasson, C., Thierfelder, T., Yang, Z., Hedenås, H., Johansson, M. et al. (2013)  
693 Ecosystem change and stability over multiple decades in the Swedish subarctic: Complex  
694 processes and multiple drivers. *Philosophical Transactions of the Royal Society B: Biological*  
695 *Sciences*, 368, 1–17. <https://doi.org/10.1098/rstb.2012.0488>

696 Callaway, R. M., Brooker, R. W., Choler, P., Kikvidze, Z., Lortie, C. J., Michalet, R. et al. (2002) Positive  
697 interactions among alpine plants increase with stress. *Nature*, 417, 844–848.  
698 <https://doi.org/10.1038/nature00812>

699 Carmona, C. P., & Pärtel, M. (2020) Estimating probabilistic site-specific species pools and dark  
700 diversity from co-occurrence data. *Global Ecology and Biogeography*, 30, 316–326.  
701 <https://doi.org/10.1111/geb.13203>

702 Chamberlain, S., Barve, V., Mcglinn, D., Oldoni, D., Desmet, P., Geffert, L., & Ram, K. (2021) *rgbif*:  
703 *Interface to the Global Biodiversity Information Facility API. Version 3.6.0.* Available at  
704 <https://CRAN.R-project.org/package=rgbif> [Accessed 15 May 2021]

705 Christensen, E., Christensen, B., & Christensen, S. (2021) Problems in using Beals' index to detect  
706 species trends in incomplete floristic monitoring data (Reply to Bruelheide et al. (2020)).  
707 *Diversity and Distributions*, 27, 1324–1327. <https://doi.org/10.1111/ddi.13276>

708 Cribari-Neto, F., Zeileis, A. (2010) Beta Regression in R. *Journal of Statistical Software*, 34, 1–24.

709 Crooks, J. A. (2005) Lag times and exotic species: The ecology and management of biological invasions  
710 in slow-motion. *Ecoscience*, 12, 316–329. <https://doi.org/10.2980/i1195-6860-12-3-316.1>

711 de Bello, F., Fibich, P., Zelený, D., Kopecký, M., Mudrák, O., Chytrý, M. Et al. (2016) Measuring size and  
712 composition of species pools: a comparison of dark diversity estimates. *Ecology and Evolution*,  
713 6, 4088–4101. <https://doi.org/10.1002/ece3.2169>

714 Ellenberg, H., Weber, H.E., Düll, R., Wirth, V., Werner, W. & Paulißen, D. (1991) *Zeigerwerte von*  
715 *Pflanzen in Mitteleuropa*. Scripta Geobotanica.

716 European Union, Copernicus Land Monitoring Service 2021, European Environment Agency (EEA).

717 Ewald, J. (2002) A probabilistic approach to estimating species pools from large compositional  
718 matrices. *Journal of Vegetation Science*, 13, 191–198. [https://doi.org/10.1111/j.1654-](https://doi.org/10.1111/j.1654-1103.2002.tb02039.x)  
719 [1103.2002.tb02039.x](https://doi.org/10.1111/j.1654-1103.2002.tb02039.x)

720 Finlay, R. D. (2008) Ecological aspects of mycorrhizal symbiosis: With special emphasis on the  
721 functional diversity of interactions involving the extraradical mycelium. *Journal of*  
722 *Experimental Botany*, 59, 1115–1126. <https://doi.org/10.1093/jxb/ern059>

723 Fløjgaard, C., Valdez, J. W., Dalby, L., Moeslund, J. E., Clausen, K. K., Ejrnæs, R. et al. (2020) Dark  
724 diversity reveals importance of biotic resources and competition for plant diversity across  
725 habitats. *Ecology and Evolution*, 10, 6078–6088. <https://doi.org/10.1002/ece3.6351>

726 Fox, J., & Weisberg, S. (2011). *An R companion to applied regression (2nd edition)*. SAGE Publications  
727 Inc.

728 Gijbels, P., Adriaens, D. & Honnay, O. (2012) An orchid colonization credit in restored calcareous  
729 grasslands. *Ecoscience*, 19, 21–28. <https://doi.org/10.2980/19-1-3460>

730 Gough, L., Shaver, G. R., Carroll, J., Royer, D. L., & Laundre, J. A. (2000) Vascular plant species richness  
731 in Alaskan arctic tundra: The importance of soil pH. *Journal of Ecology*, 88, 54–66.  
732 <https://doi.org/10.1046/j.1365-2745.2000.00426.x>

733 Guisan, A., & Thuiller, W. (2005) Predicting species distribution: Offering more than simple habitat  
734 models. *Ecology Letters*, 8, 993–1009. <https://doi.org/10.1111/j.1461-0248.2005.00792.x>

735 Haesen, S., Lembrechts, J. J., De Frenne, P., Lenoir, J., Aalto, J., Ashcroft, M. et al. (2021) ForestTemp  
736 Sub-canopy microclimate temperatures of European forests. *Global Change Biology*, 27, 6307–  
737 6319. <https://doi.org/10.1111/gcb.15892>

738 Hartig, F. (2018) *Yes, statistical errors are slowing down scientific progress! Theoretical ecology.*

739 Available at [https://theoreticalecology.wordpress.com/2018/05/03/yes-statistical-errors-are-](https://theoreticalecology.wordpress.com/2018/05/03/yes-statistical-errors-are-slowing-down-scientific-progress/)  
740 [slowing-down-scientific-progress/](https://theoreticalecology.wordpress.com/2018/05/03/yes-statistical-errors-are-slowing-down-scientific-progress/) [Accessed 2 November 2022]

741 Hartig, F. (2022) *DHARMA: Residual diagnostics for hierarchical (multi-level / mixed) regression*  
742 *Models. R package version 0.4.5.* Available at <https://CRAN.R-project.org/package=DHARMA>  
743 [Accessed 14 November 2021]

744 Hijmans, R. J., van Etten, J. (2012) *Raster: Geographic data analysis and modeling. R package version*  
745 *3.6-3.* Available at <http://CRAN.R-project.org/package=raster> [Accessed 5 October 2021]

746 Hooper, D. U., Adair, E. C., Cardinale, B. J., Byrnes, J. E. K., Hungate, B. A., Matulich, K. L. et al. (2012)  
747 A global synthesis reveals biodiversity loss as a major driver of ecosystem change. *Nature*, 486,  
748 105–108. <https://doi.org/10.1038/nature11118>

749 Howe, F., & Smallwood, J. (1982) Ecology of seed dispersal. *Annual Review of Ecology and Systematics*,  
750 *13*, 201–228. <https://doi.org/10.1146/annurev.es.13.110182.001221>

751 Jonasson, S. (1988) Evaluation of the point intercept method for the estimation of plant biomass.  
752 *Oikos*, 52, 101–106.

753 Jones, N. T., & Gilbert, B. (2016) Biotic forcing: the push–pull of plant ranges. *Plant Ecology*, 217, 1331–  
754 1344. <https://doi.org/10.1007/s11258-016-0603-z>

755 Karger, D. N., Conrad, O., Böhrner, J., Kawohl, T., Kreft, H., Soria-Auza, R. W. et al. (2017) Climatologies  
756 at high resolution for the Earth land surface areas. *Scientific Data*, 4, 170122.  
757 <https://doi.org/10.1038/sdata.2017.122>

758 Keddy, P. A. (1992) Assembly and response rules: two goals for predictive community ecology. *Journal*  
759 *of vegetation science*, 3, 157–164. <https://doi.org/10.2307/3235676>

760 Keitt, T., Bivand, R., Pebesma, E. & Rowlingson, B. (2010) *rgdal: Bindings for the Geospatial Data*  
761 *Abstraction Library. Version 1.6-5.* Available at: <https://CRAN.R-project.org/package=rgdal>  
762 [Accessed 28 March 2023]

763 Klanderud, K. (2010) Species recruitment in alpine plant communities: The role of species interactions  
764 and productivity. *Journal of Ecology*, 98, 1128–1133. [https://doi.org/10.1111/j.1365-](https://doi.org/10.1111/j.1365-2745.2010.01703.x)  
765 [2745.2010.01703.x](https://doi.org/10.1111/j.1365-2745.2010.01703.x)

766 Kleyer, M., Bekker, R. M., Knevel, I. C., Bakker, J. P., Thompson, K., Sonnenschein, M. et al. (2008) The  
767 LEDA traitbase: a database of life- history traits of the northwest European flora. *Journal of*  
768 *Ecology*, 96, 1266–1274. <https://doi.org/10.1111/j.1365-2745.2008.01430.x>

769 Kopecký, M., Macek, M., & Wild, J. (2021) Science of the Total Environment Topographic Wetness  
770 Index calculation guidelines based on measured soil moisture and plant species composition.  
771 *Science of the Total Environment*, 757, 143785.  
772 <https://doi.org/10.1016/j.scitotenv.2020.143785>

773 Körner, C. (2021) *Alpine plant life: Functional plant ecology of high mountain ecosystems*, 3rd edition.  
774 Springer Nature Switzerland AG 2021. <https://doi.org/10.1007/978-3-030-59538-8>

775 Kullman, L. (2015) Recent and past trees and climates at the Arctic/Alpine margin in Swedish Lapland:  
776 An Abisko case study Review. *Journal of Biodiversity Management & Forestry*, 4, 1–12.  
777 [doi:10.4172/2327-4417.1000150](https://doi.org/10.4172/2327-4417.1000150)

778 Legendre P, Legendre J (1998) *Numerical Ecology*, 3rd edition. Elsevier, Amsterdam.

779 Lembrechts, J. J., Lenoir, J., Nuñez, M. A., Pauchard, A., Geron, C., Bussé, G. et al. (2018) Microclimate  
780 variability in alpine ecosystems as stepping stones for non-native plant establishment above  
781 their current elevational limit. *Ecography*, 41, 900–909. <https://doi.org/10.1111/ecog.03263>

782 Lembrechts, J. J., Lenoir, J., Roth, N., Hattab, T., Milbau, A., Haider, S. et al (2019) Comparing  
783 temperature data sources for use in species distribution models: From in-situ logging to  
784 remote sensing. *Global Ecology and Biogeography*, 28, 1578–1596.  
785 <https://doi.org/10.1111/geb.12974>

786 Lembrechts, J. J., Milbau, A., & Nijs, I. (2014) Alien roadside species more easily invade alpine than



787 lowland plant communities in a subarctic mountain ecosystem. *PLoS ONE*, 9, 1–10.  
788 <https://doi.org/10.1371/journal.pone.0089664>

789 Lembrechts, J. J., Aalto, J., Ashcroft, M. B., De Frenne, P., Kopecký, M., Lenoir, J. et al. (2020) SoilTemp:  
790 A global database of near-surface temperature. *Global Change Biology*, 26, 6616–6629.  
791 <https://doi.org/10.1111/gcb.15123>

792 Lembrechts, J. J., van den Hoogen, J., Aalto, J., Ashcroft, M., De Frenne, P., Kempainen, J. et al (2021)  
793 Global maps of soil temperature. *Global Change Biology*, 28, 3110–3144.  
794 <https://doi.org/10.1111/gcb.16060>

795 Lenoir, J., Gégout, J. C., Guisan, A., Vittoz, P., Wohlgemuth, T., Zimmermann, N. E. et al. (2010) Cross-  
796 scale analysis of the region effect on vascular plant species diversity in southern and northern  
797 European mountain ranges. *PLoS One*, 5, e15734.  
798 <https://doi.org/10.1371/journal.pone.0015734>

799 Lenth, R. (2022) *Emmeans: Estimated marginal means, aka least-squares means. Version 1.8.2.*  
800 Available at: <https://CRAN.R-project.org/package=emmeans> [Accessed 14 November 2021]

801 Leroy, B., Delsol, R., Hugueny, B., Meynard, C. N., Barhoumi, C., Barbet-Massin, M., & Bellard, C. (2018)  
802 Without quality presence–absence data, discrimination metrics such as TSS can be misleading  
803 measures of model performance. *Journal of Biogeography*, 45, 1994–2002.  
804 <https://doi.org/10.1111/jbi.13402>

805 Lewis, R. J., de Bello, F., Bennett, J. A., Fibich, P., Finerty, G. E., Götzenberger, L. et al. (2017) Applying  
806 the dark diversity concept to nature conservation. *Conservation Biology*, 31, 40–47.  
807 <https://doi.org/10.1111/cobi.12723>

808 Lewis, R. J., Szava-Kovats, R., & Pärtel, M. (2016) Estimating dark diversity and species pools: An  
809 empirical assessment of two methods. *Methods in Ecology and Evolution*, 7, 104–113.  
810 <https://doi.org/10.1111/2041-210X.12443>

811 Lindén, E., Gough, L., & Olofsson, J. (2021) Large and small herbivores have strong effects on tundra  
812 vegetation in Scandinavia and Alaska. *Ecology and Evolution*, 11, 12141–12152.  
813 <https://doi.org/10.1002/ece3.7977>

814 Lüdecke, D., Ben-Shachar, M., Patil, I., Waggoner, P. & Makowski, D. (2021) “performance: An R  
815 package for assessment, comparison and testing of statistical models.” *Journal of Open Source*  
816 *Software*, 6, 3139. <https://doi.org/10.21105/joss.03139>

817 MacDougall, A. S., Caplat, P., Olofsson, J., Siewert, M. B., Bonner, C., Esch et al. (2021)  
818 Comparison of the distribution and phenology of Arctic Mountain plants between the early  
819 20th and 21st centuries. *Global Change Biology*, 27, 5070–5083.  
820 <https://doi.org/10.1111/gcb.15767>

821 Meyer, C., Weigelt, P., & Kreft, H. (2016) Multidimensional biases, gaps and uncertainties in global  
822 plant occurrence information. *Ecology Letters*, 19, 992–1006.  
823 <https://doi.org/10.1111/ele.12624>

824 Moeslund, J. E., Brunbjerg, A. K., Clausen, K. K., Dalby, L., Fløjgaard, C., Juel, A., & Lenoir, J. (2017)  
825 Using dark diversity and plant characteristics to guide conservation and restoration. *Journal of*  
826 *Applied Ecology*, 54, 1730–1741. <https://doi.org/10.1111/1365-2664.12867>

827 Mohd, M. H., Murray, R., Plank, M. J., & Godsoe, W. (2016). Effects of dispersal and stochasticity on  
828 the presence–absence of multiple species. *Ecological Modelling*, 342, 49–59.  
829 <https://doi.org/10.1016/j.ecolmodel.2016.09.026>

830 Mooney, H., Larigauderie, A., Cesario, M., Elmquist, T., Hoegh-Guldberg, O., Lavorel, S. et al. (2009)  
831 Biodiversity, climate change, and ecosystem services. *Current Opinion in Environmental*  
832 *Sustainability*, 1, 46–54. <https://doi.org/10.1016/j.cosust.2009.07.006>

833 Mossberg, B. & Stenberg, L. (2008) *Fjällflora: Sverige, Finland, Norge, Svalbard*. Wahlström &  
834 Widstrand.

835 Newbold, T., Hudson, L. N., Hill, S. L. L., Contu, S., Lysenko, I., Senior, R. A. et al. (2015) Global effects  
836 of land use on local terrestrial biodiversity. *Nature*, 520, 45–50.  
837 <https://doi.org/10.1038/nature14324>

838 Oksanen, J., Blanchet, F.G., Kindt, R. et al. (2022) *Vegan: Community ecology package. Version 2.6-4*.  
839 Available at: <https://CRAN.R-project.org/package=vegan> [Accessed 2 November 2022]

840 Ozinga, W. A., Hennekens, S. M., Schaminée, J. H. J., Bekker, R. M., Prinzing, A., Bonn, S. et al. (2005)  
841 Assessing the relative importance of dispersal in plant communities using an ecoinformatics  
842 approach. *Folia Geobotanica*, 40, 53–67. <https://doi.org/10.1007/BF02803044>

843 Parolo, G., Rossi, G., & Ferrarini, A. (2008). Toward improved species niche modelling: *Arnica montana*  
844 in the Alps as a case study. *Journal of Applied Ecology*, 45, 1410–1418.  
845 <https://doi.org/10.1111/j.1365-2664.2008.01516.x>

846 Pärtel, M. (2014) Community ecology of absent species: Hidden and dark diversity. *Journal of*  
847 *Vegetation Science*, 25, 1154–1159. <https://doi.org/10.1111/jvs.12169>

848 Pärtel, M., Carmona, C. P., Zobel, M., Moora, M., Riibak, K., & Tamm, R. (2019) DarkDivNet – A global  
849 research collaboration to explore the dark diversity of plant communities. *Journal of*  
850 *Vegetation Science*, 30, 1039–1043. <https://doi.org/10.1111/jvs.12798>

851 Pärtel, M., Szava-Kovats, R., & Zobel, M. (2011) Dark diversity: Shedding light on absent species. *Trends*  
852 *in Ecology and Evolution*, 26, 124–128. <https://doi.org/10.1016/j.tree.2010.12.004>

853 Pärtel, M., Szava-Kovats, R., & Zobel, M. (2013) Community completeness: Linking local and dark  
854 diversity within the species pool concept. *Folia Geobotanica*, 48, 307–317.  
855 <https://doi.org/10.1007/s12224-013-9169-x>

856 Pebesma, E. J., Bivand, R. S. (2005) Classes and methods for spatial data in R. *R news*, 5, 9–13.

857 Pellissier, L., Bräthen, K. A., Pottier, J., Randin, C. F., Vittoz, P., Dubuis, A. et al. (2010) Species  
858 distribution models reveal apparent competitive and facilitative effects of a dominant species  
859 on the distribution of tundra plants. *Ecography*, 33, 1004–1014.  
860 <https://doi.org/10.1111/j.1600-0587.2010.06386.x>

861 Pollock, L. J., Tingley, R., Morris, W. K., Golding, N., O'Hara, R. B., Parris, K. M. et al. (2014)  
862 Understanding co-occurrence by modelling species simultaneously with a Joint Species  
863 Distribution Model (JSDM). *Methods in Ecology and Evolution*, 5, 397–406.  
864 <https://doi.org/10.1111/2041-210X.12180>

865 QGIS Development Team. (2021) QGIS geographic information system. Open Source Geospatial  
866 Foundation Project. Available from: <http://www.qgis.org>

867 R Core Team (2021) R: A language and environment for statistical computing. R Foundation for  
868 Statistical Computing, Vienna, Austria. Available at: <https://www.R-project.org/>

869 Rashid, I., Haq, S. M., Lembrechts, J. J., Khuroo, A. A., Pauchard, A., & Dukes, J. S. (2021) Railways  
870 redistribute plant species in mountain landscapes. *Journal of Applied Ecology*, 58, 1967–1980.  
871 <https://doi.org/10.1111/1365-2664.13961>

872 Riibak, K., Reitalu, T., Tamm, R., Helm, A., Gerhold, P., Znamenskiy, S. et al. (2015) Dark diversity in  
873 dry calcareous grasslands is determined by dispersal ability and stress-tolerance. *Ecography*,  
874 38, 713–721. <https://doi.org/10.1111/ecog.01312>

875 Sonesson, M., & Lundberg, B. (1974) Late Quaternary forest development of the Tornetrask area,  
876 North Sweden. *Oikos*, 25, 121–133. <https://doi.org/10.2307/3543947>

877 Soudzilovskaia, N. A., Vaessen, S., Barcelo, M., He, J., Rahimlou, S., Abarenkov, K. et al. (2020)  
878 FungalRoot: global online database of plant mycorrhizal associations. *New Phytologist*, 227,  
879 955–966. <https://doi.org/10.1111/nph.16569>

880 Stephenson, I. (2016) *What is Dark Diversity?* Methods blog. Available at  
881 <https://methodsblog.com/2016/05/22/dark-diversity/> [Accessed 4 April 2022]

882 Tendersoo, L. (Ed) (2017) *Biogeography of Mycorrhizal Symbiosis*, 1st edition. Springer International

- 883 Publishing 2017. <https://doi.org/10.1007/978-3-319-56363-3>
- 884 Tessarolo, G., Rangel, T. F., Araújo, M. B., & Hortal, J. (2014) Uncertainty associated with survey design  
885 in Species Distribution Models. *Diversity and Distributions*, 20, 1258–1269.  
886 <https://doi.org/10.1111/ddi.12236>
- 887 Tilman, D., Isbell, F., & Cowles, J. M. (2014) Biodiversity and ecosystem functioning. *Annual Review of*  
888 *Ecology, Evolution, and Systematics*, 45, 471–493. [https://doi.org/10.1146/annurev-ecolsys-](https://doi.org/10.1146/annurev-ecolsys-120213-091917)  
889 [120213-091917](https://doi.org/10.1146/annurev-ecolsys-120213-091917)
- 890 Trindade, D. P., Carmona, C. P., Reitalu, T., & Pärtel, M. (2023) Observed and dark diversity dynamics  
891 over millennial time scales: fast life-history traits linked to expansion lags of plants in northern  
892 Europe. *Proceedings of the Royal Society B*, 290, 20221904.  
893 <https://doi.org/10.1098/rspb.2022.1904>
- 894 Tybirk, K., Nilsson, M. C., Michelsen, A., Kristensen, H. L., Sheytsova, A., Strandberg, M. T. et al. (2000)  
895 Nordic *Empetrum* dominated ecosystems: Function and susceptibility to environmental  
896 changes. *Ambio*, 29, 90–97. <https://doi.org/10.1579/0044-7447-29.2.90>
- 897 Vonlanthen, C. M., Kammer, P. M., Eugster, W., Bühler, A., & Veit, H. (2006) Alpine vascular plant  
898 species richness: The importance of daily maximum temperature and pH. *Plant Ecology*, 184,  
899 13–25. <https://doi.org/10.1007/s11258-005-9048-5>
- 900 Wedegärtner, R. E., Lembrechts, J. J., van der Wal, R., Barros, A., Chauvin, A., Janssens et al. (2022)  
901 Hiking trails shift plant species' realized climatic niches and locally increase species richness.  
902 *Diversity and Distributions*, 28, 1416-1429 <https://doi.org/10.1111/ddi.13552>
- 903 Westoby, M. (1998) A leaf-height-seed ( LHS ) plant ecology strategy scheme. *Plant and Soil*, 199, 213–  
904 227. <https://doi.org/10.1023/A:1004327224729>
- 905 Wiegmans, D., Larson, K., Clavel, J., Spreeuwens, J., Pirée, A., Nijs, I., & Lembrechts, J. (2023) Historic  
906 disturbance events may overrule climatic factors as drivers of ruderal species distributions in  
907 the Scandinavian mountains. *Authorea Preprints*. 10.22541/au.167515746.69858832/v1
- 908 Wunderlich, R. F., Lin, Y. P., Anthony, J., & Petway, J. R. (2019) Two alternative evaluation metrics to  
909 replace the true skill statistic in the assessment of species distribution models. *Nature*  
910 *Conservation*, 35, 97-116.

911

## 912 **Appendices**

913 Appendix S1. Details online data collection

914 Appendix S2. Additional results

915 Appendix S3. Contrast tests mycorrhizal associations